Drying Technology

An International Journal

ISSN: (Print) (Online) Journal homepage: https://www.tandfonline.com/loi/ldrt20

Application of ultrasound in regeneration of silica gel for industrial gas drying processes

Hooman Daghooghi-Mobarakeh, Mark Miner, Liping Wang, Robert Wang & Patrick E. Phelan

To cite this article: Hooman Daghooghi-Mobarakeh, Mark Miner, Liping Wang, Robert Wang & Patrick E. Phelan (2021): Application of ultrasound in regeneration of silica gel for industrial gas drying processes, Drying Technology, DOI: 10.1080/07373937.2021.1929296

To link to this article: https://doi.org/10.1080/07373937.2021.1929296

Published online: 01 Jun 2021.

DRYING TECHNOLOGY
https://doi.org/10.1080/07373937.2021.1929296

Application of ultrasound in regeneration of silica gel for industrial gas drying processes

Hooman Daghooghi-Mobarakeh[a], Mark Miner[b], Liping Wang[a], Robert Wang[a], and Patrick E. Phelan[a]

[a]School for Engineering of Matter, Transport & Energy, Arizona State University, Tempe, AZ, USA; [b]School of Earth and Space Exploration, Arizona State University, Tempe, AZ, USA

ABSTRACT

Industrial gas dehumidification contributes to a considerable portion of the total industrial energy consumption. Depending on the desired level of dryness, solid desiccants can be a more suitable dehumidification method compared to the conventional dehumidification processes. In this study, the ultrasound-enhanced regeneration of silica gel as a substitute to conventional heating methods is investigated. To analyze the energy-savings effect of applying ultrasound a method of constant total power levels of 20 and 25 (W) corresponding to total specific power levels of 327 and 409 (W/kg_{SG}) was adopted and for each Watt of applied ultrasonic power, the same amount was deducted from thermal power. The moisture content and regeneration temperature were measured and compared in ultrasound-assisted and non-ultrasound (heat-only) regeneration processes. Experimental results showed that applying ultrasound along with thermal power improves the regeneration process and reduces the energy required to regenerate silica gel by as much as 26%. Various transport modes contributing to mass diffusion in porous media are analyzed and an apparent diffusion coefficient for porous media that includes ultrasonication effects is proposed. Regarding regeneration temperature, with application of ultrasound, regeneration at lower temperatures by as much as ~11% was achieved.

ARTICLE HISTORY
Received 30 March 2021
Revised 5 May 2021
Accepted 10 May 2021

KEYWORDS
Dehumidification; drying; diffusion; regeneration; silica gel; ultrasound

Introduction

The dehydration of industrial gases is an essential process to prevent undesired condensation and ice formation, solid hydrate formation, hydrolysis and corrosion.[1–3] The dehydration and drying processes of industrial gases such as natural gas, compressed air, nitrogen and oxygen, that is, reducing the water vapor content of the industrial gases to a satisfactory level, are considered energy intensive.[4,5] It's estimated that about 0.5 Quads of energy was used just for natural gas and compressed air drying in 2019 in the U.S., out of a total industrial primary energy consumption of 32.5 Quads which corresponds to about 1.5%.[6,7] Currently, industrial gas dehydration is achieved by means of condensation, liquid desiccants, and solid desiccants.[3,8] Condensation dehydration is achieved either by reducing the temperature of the gas below the dewpoint (saturation temperature corresponding to the desired moisture content) and reheating the gas or by decreasing the pressure using expansion valves (Joule-Thompson effect). Compared to desiccant dehydration, condensation dehydration is the most energy-intensive drying process except for very high gas pressures (>20 MPa).[8] Liquid-desiccant dehydration is achieved by bubbling the gas through a liquid that has high affinity for water vapor. The water vapor is removed from the gas by absorption. Liquid desiccants offer the least energy-intensive drying process, however they cannot deliver the 'bone dry' gas required in some applications such as cryogenics. Commercially available liquid desiccants is either highly corrosive such as lithium chloride and lithium bromide, or prone to contamination such as glycols.[3,9] In addition, there is the major health concern of droplet/vapor carry over associated with dehydration using liquid desiccants.[10] Solid desiccant dehumidification is achieved by passing moist gas through a packed bed containing adsorbent. Since adsorbents have high affinity for water vapor, the water vapor is adsorbed on the surface of the desiccant to a certain degree, after which the material becomes saturated and needs to be regenerated. Solid desiccant dehydration energy intensity is higher than dehydration using liquid desiccants, but much lower than dehydration

CONTACT Patrick E. Phelan phelan@asu.edu

Table 1. Physical properties of silica gel.

Average bead diameter (mm)	3.5
Pore diameter (nm)	2–3
Specific surface area (m^2/g)	650
Density (kg/m^3)	700

by condensation.[11] Despite their higher energy intensity, solid desiccants are often preferable to liquid desiccants in drying processes as they can deliver much higher levels of dryness and require much simpler reactors.[1,2,12,13]

On the other hand, the downside of using solid desiccants is the lengthy and energy-intensive process of the regeneration stage, necessitating more energy-efficient regeneration processes besides just conventional heating.[14] Ultrasound inherently enhances heat and mass transfer and has been used to improve heat and mass transfer in many regeneration, drying and separation processes.[15–24] In this study the outcomes of ultrasound integration on moisture removal from silica gel from an energy efficiency perspective is investigated since the total input power in no-ultrasound (heat-only) and ultrasound-assisted regeneration processes is kept constant. Transport modes in porous media are analyzed and a modified diffusion coefficient for porous media under ultrasonic radiation is proposed. In addition, the changes in regeneration temperature under ultrasonication are analyzed to assess the possibility of ultrasound application in low-grade heat, waste heat and renewable energy utilization.

Experimental setup and procedure

Silica gel

The silica gel used in this study was procured from the Delta Adsorbents Division of Delta Enterprises, Inc. The physical and porous properties provided by the manufacturer are shown in Table 1.

Experimental procedure

Figure 1 shows a schematic diagram of the experimental setup. The main elements of the experimental setup are a power supply and cartridge heater to supply and regulate the thermal power input, a function generator, an ultrasonic amplifier, an oscilloscope, and a shunt resistor to regulate and measure the ultrasonic power input and a desorption bed. The bed is of hollow cylindrical shape of 10 cm height and 7.5 cm internal diameter with wall and bottom thicknesses of 0.25 cm and 1 cm respectively, machined out of aluminum 6061. The regeneration temperature of the silica gel was measured using five T-type thermocouples (Omega Engineering-AWG 24) positioned radially and axially and NATIONAL INSTRUMENTS data acquisition device NI 9212. The total input power and "ultrasonic-to-total power ratios" (P_{US}/P_{Total}) are provided in Table 2. The resonant frequency of the ultrasonic transducer is 40 (kHz) provided by the supplier, however, the ultrasonic-assisted regeneration experiments were conducted at a transducer/bed assembly resonant frequency of 31.8 (kHz).

Preparation of the dried silica gel sample was achieved by heating it in an oven at 120 °C (to ensure full dryness) and controlling the mass until no change in mass was observed. The mass of the dried sample was controlled to be 61.13 ± 0.01 g in all experiments.

The dried sample was then saturated to 34% moisture content MC using an ultrasonic humidifier (Honeywell Mistmate HUL520) with R/O water, and airflow with air velocity of 0.2 ± 0.02 m/s. The moisture content MC, representing the mass of water adsorbed by silica gel, is defined as[25]:

$$MC = \frac{m_{measured} - m_{dry}}{m_{dry}} \tag{1}$$

where $m_{measured}$ is the measured mass of the sample and m_{dry} the measured mass of the dry sample. In the saturation stage, the relative humidity and the temperature of the feed flow were controlled at 95%–100% and 20 °C respectively using a Honeywell HIH-6130 temperature and relative humidity sensor. The thermocouple–data acquisition assembly was calibrated using a HONEYWELL HIH 6130 temperature sensor with an accuracy of ±0.5 °C. The mass of the bed is measured using an electronic scale (My Weigh SCMIM01) with a capacity/resolution of 1000 ± 0.01 g. The uncertainties of the mass and temperature measurements are presented in Table 3.

The uncertainties of the dependent variables are determined using[26]:

$$u_f = \sqrt{\left(u_1{}^2\left(\frac{\partial f}{\partial x_1}\right)^2 + u_2{}^2\left(\frac{\partial f}{\partial x_2}\right)^2 + u_3{}^2\left(\frac{\partial f}{\partial x_3}\right)^2 + \ldots\right)} \tag{2}$$

where u_f is the uncertainty of the dependent variable $f(x_1, x_2, x_3, \ldots)$ and $u_1, u_2, u_3, \ldots$ are the uncertainties involved in the measurement of the variables $x_1, x_2, x_3, \ldots$ respectively. The maximum values of uncertainty of the calculated variables are provided in Table 4.

For a more detailed description of the experimental setup and heat losses, see our previous work.[27]

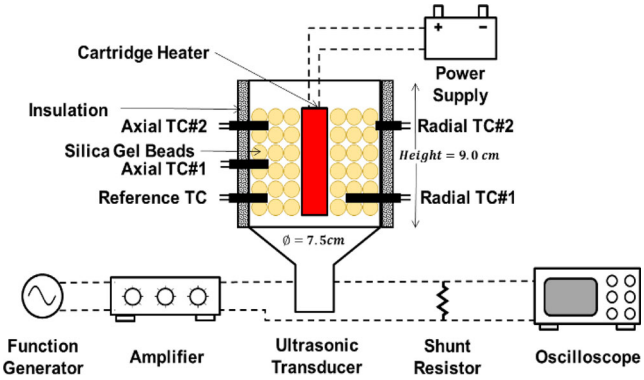

Figure 1. Schematic diagram of the experimental setup.

Table 2. Total power levels and power combinations.

P_{Total} (W)	P_{TH} (W)	P_{US} (W)	P_{US}/P_{Total}
20	20	0	0
20	15	5	0.25
20	10	10	0.50
25	25	0	0
25	20	5	0.20
25	15	10	0.40

Table 3. Accuracy of measured variables.

Measured variable	Uncertainty	Unit
Temperature	±0.05	°C
Mass	±0.01	g
Voltage	1	%
Phase angle	0.1	Minute

Table 4. Maximum values of uncertainty for the calculated variables.

Dependent variable	Maximum uncertainty	Unit
MC	±0.21	%
μ	±0.37	%
T_{reg}	±1.12	°C
UDEE	±2.11	%

Results and discussion

Moisture removal

The variation of the silica gel *MC* with time for all experiments is depicted in Figure 2. To establish the influence of ultrasound in the regeneration process, the *dimensionless moisture removed* μ is defined:

$$\mu = \frac{m_{ini} - m_{measured}}{m_{ini} - m_{dry}} \tag{3}$$

where m_{ini} is the initial mass of the sample (adsorbent + adsorbate).

The specific regenerating power of the silica gel-water pair is reported to be about 180–390 W_{th}/kg_{SG}, so the 20 and 25 W of total input power corresponding to specific desorbing input powers of 327 and 409 W/kg_{SG} respectively, are comparable.[28,29] It can be inferred from Figure 2 that at both total power levels P_{Total} = 20 or 25 W, at any value of the ratio P_{US}/P_{Total}, application of

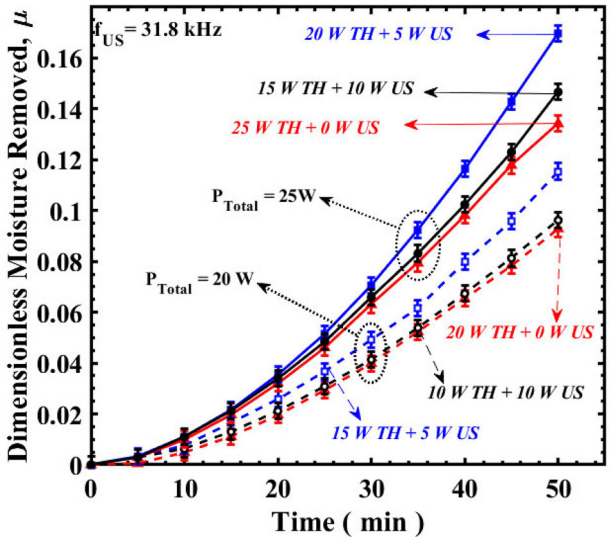

Figure 2. Variation of dimensionless moisture removed in ultrasound-assisted and heat-only regeneration of silica gel.

ultrasound improves the moisture removal from silica gel. The observed trend is that while the total input power to the desorption bed remains constant, replacing smaller portions of thermal power i.e., 20% (20 W TH + 5 W US) and 25% (15 W TH + 5 W US) with ultrasonic power significantly enhances moisture removal compared to the no-ultrasound desorption process at the same total power level. At higher P_{US}/P_{Total} of 40% (15 W TH + 10 W US) and 50% (10 W TH + 10 W US), the observed enhancement associated with integration of ultrasound is still perceptible, however not as significant as at lower P_{US}/P_{Total}. Since there is no increase in the total input power to the system, the observed improvement must be ultrasound-induced. Although many mechanisms such as surface cavitation, pulsating partial vacuum, pressure alteration, acoustic dissipation, adsorbent surface energy alteration, enhanced mass transfer and sonic currents have proposed, the fundamental mechanisms behind why the integration of ultrasound enhances regeneration are still not clear.[27,30,31] The regeneration of desiccants can be considered to

consist of two processes: the detachment of the adsorbate molecule from the adsorbent surface (desorption) and transport of the detached adsorbate molecule out of the pore and eventually far from the surface (diffusion). It's worth mentioning that mechanisms such as pulsating partial vacuum, pressure alteration and adsorbent surface energy alteration have been proposed to be the key players in ultrasound-enhanced desorption processes.[27,30,31] The diffusion mechanism of a single adsorbate molecule in porous media is described through Knudsen diffusion, slip diffusion, surface diffusion and viscous diffusion.[30,32] Depending on many parameters such as adsorbent saturation degree, adsorbent pore size, pressure and temperature, one or all of these mechanisms contribute to mass transfer either in series or parallel.[30,33,34] Yao et al. reported that for porous media with pore diameter less than 200 Å which includes zeolites, activated alumina and silica gel, the ultrasound-enhanced mass transfer is due to the effect of temperature rise, induced by acoustic dissipation, on diffusivity.[30] Since the acoustic dissipation increases with an increase in frequency, ultrasound-enhanced mass transfer should therefore increase with increasing ultrasonic frequency.[27,35–38] This hypothesis, however, contradicts the experimental results of previous work in which the ultrasound-enhanced regeneration of silica gel, zeolite 13X and activated alumina was found to be inversely proportional to ultrasonic frequency, and with an increase in frequency the ultrasound-induced enhancement noticeably diminished.[27,38] In nano-porous materials the transport mechanism is determined using the Knudsen number k_n.[32,39] The mean free path Λ is determined as[40]:

$$\Lambda = \frac{k_B T}{\pi\sqrt{2} P d^2} \tag{4}$$

where k_B is the Boltzmann constant, T temperature, P pressure and d the molecule effective diameter. For water molecules under normal conditions ($P = 1$ atm and $T = 300$ K) the mean free path is about 0.128 µm. Considering an average pore diameter of $d_p \cong 2.5$ nm for silica gel, $k_n = \Lambda/d_p \cong 50$, meaning that the probability of molecule-molecule collisions is negligible compared to molecule-wall collisions, thus justifying Knudsen diffusion.[32,39] When the transport occurs inside relatively large pores, under ultrasonic radiation when the pressure drastically alters periodically and upon increase reduces the mean free path and consequently reduces k_n, the diffusion mechanism changes to transitional Knudsen-viscous (slip) and eventually fully viscous diffusion.[32] The advective-diffusive model (ADM) and the dusty-gas model (DGM), based on Knudsen, transition, and viscous transport modes, have been proposed to model the combined gas phase diffusion and advection in porous media. Under atmospheric pressure and for porous media with relatively high permeabilities ($k > 10^{-13}$ m^2), both models are in good agreement.[41] The diffusivity, D_{ADM}, based on ADM disregarding the binary transport mode is defined as[41]:

$$D_{ADM} = \frac{k_0}{\nu_g}\left(1 - \frac{b}{P}\right) RT \tag{5}$$

where k_0 is the intrinsic permeability, ν_g the gas-phase kinematic viscosity, b the Klingenberg factor (slip and Knudsen diffusion correction factor), P the gas-phase pressure, R the ideal gas constant and T the temperature. This model, however, is more suitable for porous media of low surface area such as soil, rock and shale as it disregards surface diffusion.[33,41] For sorbents of high surface area such as activated carbon and silica gel surface diffusion is regarded as the most important mode of transport and experimentally it has been shown that the apparent diffusivity is one order of magnitude higher than the calculated pore diffusion (surface diffusion excluded) which contributes to surface diffusion.[32,42–44] Many parameters such as surface coverage, surface temperature and activation energy affect the surface diffusivity D_s which can be written as[32,42]:

$$D_s = D_{s,\infty}(\theta)\ e^{(-E_{ac}/RT)} \tag{6}$$

where $D_{s,\infty}(\theta)$ is the concentration-dependent surface diffusivity at infinite temperature, θ the surface coverage, and E_{ac} the activation energy. The activation energy E_{ac} is a fraction of the adsorption energy $E_{ad} = f(A_{ads})$ which itself is a function of adsorption/desorption potential[42,45–47]:

$$E_{ac} = \alpha\, f(A_{ads})\ \ 0 < \alpha \leq 1 \tag{7}$$

where α is a ratio that depends on the adsorbate-adsorbent interactions, f an arbitrary function and A_{ads} the adsorption potential defined as[48,49]:

$$A_{ads} = RTln\left(\frac{P_s}{P}\right) \tag{8}$$

where P_s is the adsorbate saturation pressure at T. The total diffusivity D_T that includes Knudsen, slip, viscous and surface diffusion mechanisms can thus be represented as:

$$D_T = \frac{k_0}{\nu_g}\left(1 - \frac{b}{P}\right) RT + D_{s,\infty}(\theta)\ \exp\left[-\ \frac{\alpha f\left(RTln\left(\frac{P_s}{P}\right)\right)}{RT}\right] \tag{9}$$

Under ultrasonic radiation, pressure varies periodically[50]:

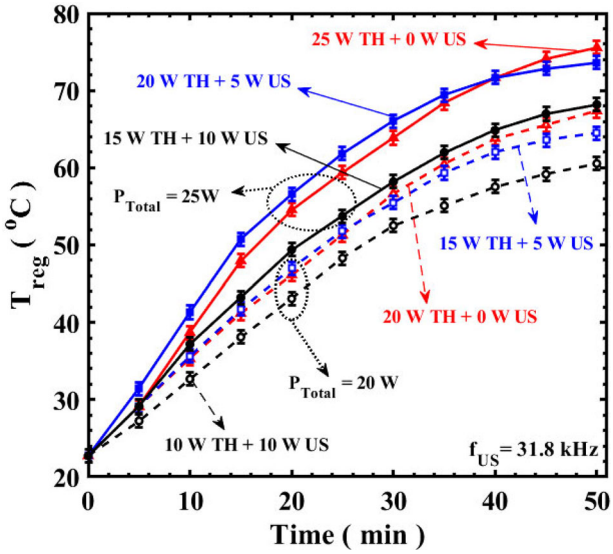

Figure 3. Measured regeneration temperature of silica gel.

$$P(t) = P_\infty + P_a \sin(\omega t) \tag{10}$$

where P_∞ is the ambient pressure, P_a the pressure amplitude, and ω the angular frequency. Substituting alternating pressure into Eq. (9) yields the apparent diffusion coefficient D_{app} in porous media under ultrasonic radiation:

$$D_{app} = \frac{k_0}{\nu_g}\left(1 - \frac{b}{P_\infty + P_a \sin(\omega t)}\right) RT + D_{s,\infty}(\theta)\ \exp\left[-\frac{\alpha f\left(RT ln\left(\frac{P_s}{P_\infty + P_a \sin(\omega t)}\right)\right)}{RT}\right] \tag{11}$$

Equation (11) represents the contributions of various diffusion mechanisms–regardless of whether they are in series or parallel–and suggests the dependency of D_{app} on temperature, ultrasonic pressure and ultrasonic frequency for a given porous medium as previously observed.[27,31,38,51] D_{app} increases with an increase in temperature and since the temperature rise due to the acoustic dissipation is insignificant, increases only with increasing thermal power. Additionally, the pressure alteration induced by ultrasound waves during rarefaction (low-pressure zones) results in an increase in apparent diffusivity. The magnitude of the pressure reduction is proportional to the ultrasonic intensity I by a power of 0.5[52]:

$$P_a = \sqrt{2\rho c I} \tag{12}$$

where ρ is the density of the medium and c the speed of sound. The dependency of D_{app} on the ultrasonic frequency is described through the time period of sound waves. With an increase in frequency, the pressure alteration becomes so fast that there is not enough time for low pressure zones to effectively be established.[27,53,54]

Regeneration temperature

The variation of silica gel regeneration temperature, T_{reg}, averaged over five measured temperatures at various radial and axial locations with time is depicted in Figure 3. The temperature of the silica gel during the regeneration process is dictated by three factors namely heat input, acoustic dissipation and ultrasonic-enhanced heat transfer.[55,56]

At any power level, the lowest regeneration temperature is observed at the highest P_{US}/P_{Total} ratio when a significant fraction (40% at 25 W total power level and 50% at 20 W total power input) of thermal power is replaced by ultrasonic power implying that the thermal input is the leading factor in controlling the regeneration temperature regime compared to ultrasonic-enhanced heat transfer and acoustic dissipation. Also, values of T_{reg} at low ultrasonic input, i.e., high thermal input and no ultrasound including heat-only input, are observed to be very close suggesting that that when a small portion (20% at P_{Total} = 25 W and 25% at P_{Total} = 20 W) of thermal power is replaced by ultrasonic power, the ultrasound-enhanced heat transfer can nearly offset the effect of the eliminated portion of the thermal input on regeneration temperature.

Energy efficiency of ultrasound-assisted regeneration

To investigate the improved energy efficiency associated with integration of ultrasound, the metric *ultrasonic desorption efficiency enhancement UDEE* from[27] is utilized. The metric *UDEE* indicates the amount of energy saved relative to a heat-only regeneration process when a portion of the thermal power is replaced with ultrasonic power while the total power remains constant, and is defined as:

$$UDEE = \frac{\frac{P_{Total}\ \Delta t}{\Delta m_{removed,\ non\ US}} - \frac{P_{Total}\ \Delta t}{\Delta m_{removed,US}}}{\frac{P_{Total}\ \Delta t}{\Delta m_{removed,\ non\ US}}} \tag{13}$$

where P_{Total} is the total input power to the system, $\Delta m_{removed,US}$ the mass of adsorbate (water) removed in a desorption process involving ultrasound, $\Delta m_{removed,non\ US}$ the mass of adsorbate (water) removed in a heat-only desorption process and Δt the total time of the experiment (50 minutes). Figure 4 shows the values of *UDEE* for both power levels (20

and 25 W) and all P_{US}/P_{Total}. Regarding the dependence on P_{US}/P_{Total}, there is a general downward trend in *UDEE* with an increase in P_{US}/P_{Total}. Energy efficiency improvement ensues from the integration of ultrasound in any case, however, the highest energy saved, i.e., 26% is achieved at the lowest ultrasonic input—20% of the total input.

Moisture content variation with temperature

The issue with current methods of regenerating solid adsorbents is the relatively high levels of regeneration temperature requiring high thermal energy input. Utilization of low-grade thermal energy such as waste heat and solar thermal energy could potentially decrease the energy and carbon intensity of drying and dehumidification processes involving solid adsorbents. However, utilization of low-grade heat is limited by its inherent low temperature. Ultrasound, which besides temperature incorporates alternating pressure and surface energy into desorption kinetics, can alter the desorption dynamics. Figure 5 shows the variation of silica gel moisture content with regeneration temperature T_{reg}. At both power levels, relative to heat-only regeneration, integration of ultrasound decreases the regeneration temperature.

Additionally, at higher P_{US}/P_{Total}, i.e., $P_{US}/P_{Total} =$ 0.4 and 0.5, there is a noticeable drop in T_{reg}. To investigate the effect of incorporating ultrasound on the variation of *MC* with T_{reg}, the temperatures at which ultrasound-assisted and heat-only regeneration processes reach the same amount of remaining adsorbed moisture are compared. To do so, for each power level, the water content of the adsorbent at the end of the heat-only experiment is considered as the baseline value. Then the temperature to reach the same water content in ultrasound-assisted regeneration with the same total power input, is determined. The temperatures at which the *MC* reaches the baseline value for all power ratios are presented in Table 5. The lowest T_{reg} are observed at $P_{US}/P_{Total} = 0.4$ and 0.5 with 9.9% and 10.6% lower T_{reg}, respectively. Shifting toward lower P_{US}/P_{Total}, the decrease in T_{reg} compared to no-ultrasound decreases drastically. It is noteworthy that at these values of P_{US}/P_{Total} the *UDEE* values are the lowest, meaning that there is a tradeoff between lowering T_{reg} and lowering the regeneration energy intensity when it comes to utilization of ultrasound.

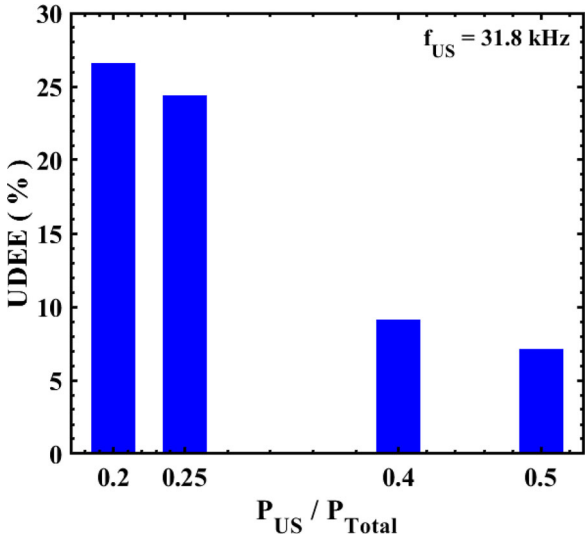

Figure 4. Ultrasonic desorption efficiency enhancement (*UDEE*) for the regeneration of silica gel. The uncertainty of *UDEE* is provided in Table 4.

Conclusion

Regeneration of silica gel under ultrasonic radiation for application in solid desiccant industrial gas drying

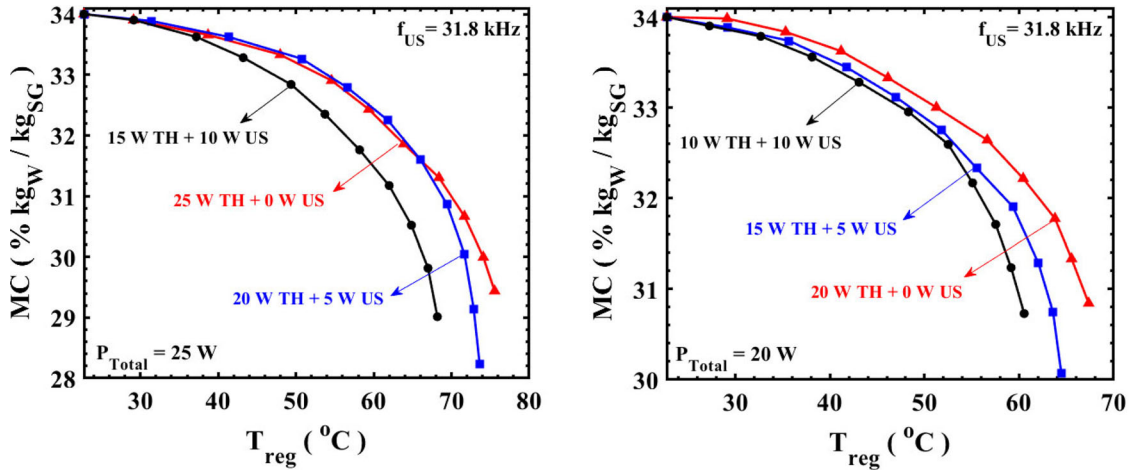

Figure 5. Moisture content variation with average regeneration temperature for silica gel, $P_{Total} = 20$ W (left) and $P_{Total} = 25$ W (right). The uncertainties of *MC* and T_{reg} are provided in Table 4.

Table 5. Regeneration temperatures to reach final moisture content, where the initial moisture content is 34% for each case.

Total power (W)	P_{US}/P_{Total}	Final moisture content (%)	T_{reg} (°C)
20	0.00	30.8	66.8
	0.25		62.8
	0.50		59.7
25	0.00	29.4	75.1
	0.20		72.4
	0.40		67.7

is investigated. Since at each power level the total power input P_{Total} was kept constant, the results of both ultrasound-assisted and non-ultrasound regeneration processes can be compared. Analyzing the values of moisture content, it can be concluded the application of ultrasound, regardless of P_{Total} or P_{US}/P_{Total} where P_{US} is the ultrasonic power, results in higher moisture removal rate. The water vapor diffusion regime in silica gel is investigated and a diffusion model that includes all likely transport modes in porous media is proposed, based on which an apparent diffusion coefficient that considers temperature and acoustic inputs is developed. Regarding the regeneration temperature, it is concluded that the regeneration temperature of the silica gel is not solely dictated by the thermal input and the ultrasound-enhanced heat transfer and acoustic dissipation noticeably contributes to the temperature rise. To appraise the energy efficiency associated with integration of ultrasound the metric ultrasonic desorption efficiency enhancement *UDEE* is used. Comparing the values of *UDEE* in ultrasound-assisted and non-ultrasound regeneration processes proves that application of ultrasound at any power level and all P_{US}/P_{Total} results in energy savings by as much as 26%. The lower P_{US}/P_{Total} are observed to be more effective in improving energy efficiency than higher P_{US}/P_{Total}. The variation of *MC* with T_{reg} is investigated and integration of ultrasound observed to lower the regeneration temperature. The highest drop in T_{reg} was achieved at highest P_{US}/P_{Total} with ∼11% lower T_{reg}.

Nomenclature

α	energy ratio (-)
ρ	density kg m^{-3}
μ	dimensionless moisture removed (-)
Λ	mean free path μm
ν_g	kinematic viscosity m^2 s^{-1}
θ	surface coverage (-)
ω	angular frequency Rad s^{-1}
$\Delta m_{removed,US}$	mas of adsorbate removed with ultrasound g
$\Delta m_{removed,non\ US}$	mas of adsorbate removed without ultrasound g
Δt	time s
A_{ads}	*adsorption potential J*
b	Klingenberg factor Pa
c	speed of sound m s^{-1}
d	molecule effective diameter nm
d_p	*pore diameter* nm
D_{ADM}	diffusivity of advective-diffusive model m^2 s^{-1}
D_{app}	apparent diffusivity m^2 s^{-1}
D_s	surface diffusivity m^2 s^{-1}
$D_{s,\infty}$	surface diffusivity at infinite temperature m^2 s^{-1}
D_T	total diffusivity m^2 s^{-1}
E_{ac}	*activation energy J*
f_{US}	ultrasonic frequency kHz
k_0	intrinsic permeability m^2
k	permeability m^2
k_B	Boltzmann constant J K^{-1}
k_n	Knudsen number (-)
I	ultrasonic intensity W m^{-2}
MC	moisture content (-)
m_{dry}	*mass of dry adsorbent g*
m_{ini}	initial mass of saturated adsorbent g
$m_{measured}$	*measured mass g*
m_s	*mass of dry adsorbent g*
P	pressure Pa
P_a	pressure amplitude Pa
P_s	saturation pressure Pa
P_∞	*ambient pressure Pa*
P_{Total}	*total power W*
P_{TH}	*thermal power W*
P_{US}	*ultrasonic power W*
R	ideal gas constant J K^{-1} mol^{-1}
T	temperature K
T_{reg}	*regeneration temperature* °C
TH	thermal (-)
$UDEE$	ultrasonic desorption efficiency enhancement (-)
US	ultrasonic (-)

Acknowledgment

This material is based upon work supported by the National Science Foundation under Grant Number CBET—1703670. Any opinions, findings, and conclusions or recommendations expressed in this material are those of the authors and do not necessarily reflect the views of the National Science Foundation.

Authors contribution

Hooman Daghooghi-Mobarakeh: Methodology, Investigation, Writing—original draft. **Mark Miner:** Conceptualization, Funding acquisition, Writing—review & editing. **Liping Wang:** Conceptualization, Funding acquisition, Writing—review & editing. **Robert Wang:** Conceptualization, Funding acquisition, Writing—review & editing. **Patrick E. Phelan:** Conceptualization, Funding acquisition, Writing—review & editing, Supervision.

References

[1] Nastaj, J.; Ambrożek, B. Modeling of Drying of Gases Using Solid Desiccants. *Dry. Technol.* **2009**, *27*, 1344–1352. DOI: 10.1080/07373930903383679.

[2] Nastaj, J.; Ambrożek, B. Modeling of Drying of Gaseous Mixtures in TSA System with Fixed Bed of Solid Desiccants. *Dry. Technol.* **2012**, *30*, 1062–1071. DOI: 10.1080/07373937.2012.685138.

[3] Gandhidasan, P.; Al-Farayedhi, A. A.; Al-Mubarak, A. A. Dehydration of Natural Gas Using Solid Desiccants. *Energy*. **2001**, *26*, 855–868. DOI: 10.1016/S0360-5442(01)00034-2.

[4] Chapas, R. B.; Colwell, J. A. Industrial Technologies Program Research Plan for Energy-Intensive Process Industries. *PNNL-17075*. **2007**, 9–11.

[5] Stakić, M.; Stefanović, P.; Cvetinović, D.; Škobalj, P. Convective Drying of Particulate Solids-Packed vs. Fluid Bed Operation. *Int. J. Heat Mass Transf.* **2013**, *59*, 66–74. DOI: 10.1016/j.ijheatmasstransfer.2012.11.078.

[6] Kinigoma, B.; Ani, G. Comparison of Gas Dehydration Methods Based on Energy Consumption. *J. Appl. Sci. Environ. Manag.* **2016**, *20*, 253–258–258.

[7] Outlook, A. E. Table 6. Industrial Sector Key Indicators and Consumption,2019.

[8] Netusil, P.; Ditl, M. Natural Gas Dehydration. *Intech.* **2012**, *13*,pp. 15-19. DOI: 10.1016/j.colsurfa.2011.12.014.

[9] Mokhatab, S.; Poe, W. A. Natural Gas Dehydration. In *Handbook of Natural Gas Transmission and Processing*; Elsevier, Gulf Professional Publishing; pp. 317–352. DOI: 10.1016/B978-0-12-386914-2.00009-1.

[10] Gurubalan, A.; Maiya, M. P.; Geoghegan, P. J. A. Comprehensive Review of Liquid Desiccant Air Conditioning System. *Appl. Energy*. **2019**, *254*, 113673. DOI: 10.1016/j.apenergy.2019.113673.

[11] Djaeni, M.; van Straten, G.; Bartels, P. V.; Sanders, J. P. M.; van Boxtel, A. J. B. Energy Efficiency of Multi-Stage Adsorption Drying for Low-Temperature Drying. *Dry. Technol.* **2009**, *27*, 555–564. DOI: 10.1080/07373930802715682.

[12] Yadav, A.; Bajpai, V. K. Experimental Comparison of Various Solid Desiccants for Regeneration by Evacuated Solar Air Collector and Air Dehumidification. *Dry. Technol.* **2012**, *30*, 516–525. DOI: 10.1080/07373937.2011.647997.

[13] Djaeni, M.; A'yuni, D. Q.; Alhanif, M.; Hii, C. L.; Kumoro, A. C. Air Dehumidification with Advance Adsorptive Materials for Food Drying: A Critical Assessment for Future Prospective. *Dry. Technol.* **2021**, 1–19. DOI: 10.1080/07373937.2021.1885042.

[14] Witkiewicz, K.; Nastaj, J. Modeling of Microwave-Assisted Regeneration of Selected Adsorbents Loaded with Water or Toluene. *Dry. Technol.* **2014**, *32*, 1369–1385. DOI: 10.1080/07373937.2014.900506.

[15] Bamasag, A.; Daghooghi-Mobarakeh, H.; Alqahtani, T.; Phelan, P. Performance Enhancement of a Submerged Vacuum Membrane Distillation (S-VMD) System Using Low-Power Ultrasound. *J. Memb. Sci.* **2021**, *621*, 119004. DOI: 10.1016/j.memsci.2020.119004.

[16] Garcia-Perez, J. V.; Carcel, J. A.; Riera, E.; Rosselló, C.; Mulet, A. Intensification of Low-Temperature Drying by Using Ultrasound. *Dry. Technol.* **2012**, *30*, 1199–1208. DOI: 10.1080/07373937.2012.675533.

[17] Muralidhara, H. S.; Ensminger, D.; Putnam, A. Acoustic Dewatering and Drying (Low and High Frequency): State of the Art Review. *Dry. Technol.* **1985**, *3*, 529–566. DOI: 10.1080/07373938508916296.

[18] Liu, B.; Wang, B.; Wang, Y.; Chitrakar, B.; Zhang, M. Effect of Ultrasound Pretreatment on Physical, Bioactive, and Antioxidant Properties of Carrot Cubes after Centrifugal Dewatering. *Dry. Technol.* **2021**, 1–12. DOI: 10.1080/07373937.2021.1874969.

[19] Baeghbali, V.; Niakousari, M.; Ngadi, M. O.; Hadi Eskandari, M. Combined Ultrasound and Infrared Assisted Conductive Hydro-Drying of Apple Slices. *Dry. Technol.* **2019**, *37*, 1793–1805. DOI: 10.1080/07373937.2018.1539745.

[20] Andrés, R. R.; Riera, E.; Gallego-Juárez, J. A.; Mulet, A.; García-Pérez, J. V.; Cárcel, J. A. Airborne Power Ultrasound for Drying Process Intensification at Low Temperatures: Use of a Stepped-Grooved Plate Transducer. *Dry. Technol.* **2021**, *39*,245–258. DOI: 10.1080/07373937.2019.1677704.

[21] Mao, F.; Han, X.; Huang, Q.; Yan, J.; Chi, Y. Effect of Frequency on Ultrasound-Assisted Centrifugal Dewatering of Petroleum Sludge. *Dry. Technol.* **2016**, *34*, 1948–1956. DOI: 10.1080/07373937.2016.1144611.

[22] Majerič, P.; Rudolf, R.; Friedrich, B.; Ternik, P. Numerical and Experimental Analysis of the Single Droplet Evaporation in a Ultrasonic Spray Pyrolysis Device. *Dry. Technol.* **2018**, *36*, 11–20. DOI: 10.1080/07373937.2017.1292520.

[23] Peng, C.; Moghaddam, S. Energy Efficient Piezoelectrically Actuated Transducer for Direct-Contact Ultrasonic Drying of Fabrics. *Dry. Technol.* **2020**, *38*, 879–888. DOI: 10.1080/07373937.2019.1596119.

[24] Zhou, C.; Cai, Z.; Wang, X.; Feng, Y.; Xu, X.; Yagoub, A. E. A.; Wahia, H.; Ma, H.; Sun, Y. Effects of Tri-Frequency Ultrasonic Vacuum-Assisted Ethanol Pretreatment on Infrared Drying Efficiency, Qualities and Microbial Safety of Scallion Stalk Slices. *Dry. Technol.* **2021**, 1–16. DOI: 10.1080/07373937.2021.1894572.

[25] Mujumdar, A. S., Ed. *Handbook of Industrial Drying*, 3rd ed.; CRC Press, Boca Raton, **2006**. DOI: 10.1201/9781420017618.

[26] Holman, J. P. *Experimental Methods for Engineers*, 7th ed.; McGraw-Hill Series in Mechanical Engineering; McGraw-Hill: Boston, **2001**.

[27] Daghooghi-Mobarakeh, H.; Campbell, N.; Bertrand, W. K.; Kumar, P. G.; Tiwari, S.; Wang, L.; Wang, R.; Miner, M.; Phelan, P. E. Ultrasound-Assisted Regeneration of Zeolite/Water Adsorption Pair. *Ultrason. Sonochem.* **2020**, *64*, February, 105042. DOI: 10.1016/j.ultsonch.2020.105042.

[28] Niazmand, H.; Talebian, H.; Mahdavikhah, M. Bed Geometrical Specifications Effects on the Performance of Silica/Water Adsorption Chillers 'Ome' Triques Du Lit Sur La Performance Effects Des Spe 'Adsorption Au Gel de Silice/Eau Des Refroidisseurs A'. *Int. J. Refrig.* **2012**, *35*, 2261–2274. DOI: 10.1016/j.ijrefrig.2012.08.017.

[29] Chang, W.; Wang, C.; Shieh, C. Experimental Study of a Solid Adsorption Cooling System Using Flat-Tube Heat Exchangers as Adsorption Bed. *Appl. Therm. Eng.* **2007**, *27*, 2195–2199. DOI: 10.1016/j.applthermaleng.2005.07.022.

[30] Yao, Y.; Liu, S. *Ultrasonic Technology for Desiccant Regeneration*; John Wiley & Sons, Incorporated, 2014.

[31] Daghooghi Mobarakeh, H.; Bandara, K.; Wang, L.; Wang, R.; Phelan, P. E.; Miner, M. Low-Grade Heat Utilization Through Ultrasound-Enhanced Desorption of Activated Alumina/Water for Thermal Energy Storage. *Power*; **2020**. DOI: 10.1115/POWER2020-16802.

[32] Do, D. D. *Adsorption Analysis: Equilibria and Kinetics; Series on Chemical Engineering*; Imperial College Press, London, 1998.

[33] Reinecke, S. A.; Sleep, B. E. Knudsen Diffusion, Gas Permeability, and Water Content in an Unconsolidated Porous Medium. *Water Resour. Res.* **2002**, *38*, 16–1–16-15. DOI: 10.1029/2002WR001278.

[34] Yao, Y. Enhancement of Mass Transfer by Ultrasound: Application to Adsorbent Regeneration and Food Drying/Dehydration. *Ultrason. Sonochem.* **2016**, *31*, 512–531. DOI: 10.1016/j.ultsonch.2016.01.039.

[35] Kerabchi, N.; Merouani, S.; Hamdaoui, O. Depth Effect on the Inertial Collapse of Cavitation Bubble under Ultrasound: Special Emphasis on the Role of the Wave Attenuation. *Ultrason. Sonochem.* **2018**, *48*, 136–150. DOI: 10.1016/j.ultsonch.2018.05.004.

[36] Amarillo, M.; Pérez, N.; Blasina, F.; Gambaro, A.; Leone, A.; Romaniello, R.; Xu, X. Q.; Juliano, P. Impact of Sound Attenuation on Ultrasound-Driven Yield Improvements during Olive Oil Extraction. *Ultrason. Sonochem.* **2019**, *53*, 142–151. DOI: 10.1016/j.ultsonch.2018.12.044.

[37] Rashwan, S. S.; Dincer, I.; Mohany, A. Investigation of Acoustic and Geometric Effects on the Sonoreactor Performance. *Ultrason. Sonochem.* **2020**, *68*, 105174. DOI: 10.1016/j.ultsonch.2020.105174.

[38] Zhang, W.; Yao, Y.; Wang, R. Influence of Ultrasonic Frequency on the Regeneration of Silica Gel by Applying High-Intensity Ultrasound. *Appl. Therm. Eng.* **2010**, *30*, 2080–2087. DOI: 10.1016/j.applthermaleng.2010.05.016.

[39] Cunningham, R. E.; Williams, R. J. *Diffusion in Gases and Porous Media*; Springer, New York, **1980**, DOI: 10.1007/978-1-4757-4983-0.

[40] Chen, G. *Nanoscale Energy Transport and Conversion: A Parallel Treatment of Electrons, Molecules, Phonons, and Photons*; Oxford University Press: Oxford; New York, **2005**.

[41] Webb, S. W.; Pruess, K. The Use of Fick's Law for Modeling Trace Gas Diffusion in Porous Media. *Transp. Porous Media* **2003**, *51*, 327–341. DOI: 10.1023/A:1022379016613.

[42] Medved', I.; Černý, R. Surface Diffusion in Porous Media: A Critical Review. *Micropor. Mesopor. Mater.* **2011**, *142*, 405–422. DOI: 10.1016/j.micromeso.2011.01.015.

[43] Miyabe, K.; Guiochon, G. Surface Diffusion in Reversed-Phase Liquid Chromatography. *J. Chromatogr. A* **2010**, *1217*, 1713–1734. DOI: 10.1016/j.chroma.2009.12.054.

[44] Miyabe, K.; Guiochon, G. Influence of the Modification Conditions of Alkyl Bonded Ligands on the Characteristics of Reversed-Phase Liquid Chromatography. *J. Chromatogr. A* **2000**, *903*, 1–12. DOI: 10.1016/S0021-9673(00)00891-8.

[45] Gilliland, E. R.; Baddour, R. F.; Perkinson, G. P.; Sladek, K. J. Diffusion on Surfaces. I. Effect of Concentration on the Diffusivity of Physically Adsorbed Gases. *Ind. Eng. Chem. Fund.* **1974**, *13*, 95–100. DOI: 10.1021/i160050a001.

[46] Sladek, K. J.; Gilliland, E. R.; Baddour, R. F.; Sladek, K. J. Diffusion on Surfaces. II. Correlation of Diffusivities of Physically and Chemically Adsorbed Species. *Ind. Eng. Chem. Fund.* **1974**, *13*, 100–105. DOI: 10.1021/i160050a002.

[47] Robell, A. J.; Ballou, E. V.; Boudart, M. Surface Diffusion of Hydrogen on Carbon. *J. Phys. Chem.* **1964**, *68*, 2748–2753. DOI: 10.1021/j100792a003.

[48] Urano, K.; Koichi, Y.; Nakazawa, Y. Equilibria for Adsorption of Organic Compounds on Activated Carbons in Aqueous Solutions I. Modified Freundlich Isotherm Equation and Adsorption Potentials of Organic Compounds. *J. Colloid Interface Sci.* **1981**, *81*, 477–485. DOI: 10.1016/0021-9797(81)90429-X.

[49] Bering, B. P.; Dubinin, M. M.; Serpinsky, V. V. Theory of Volume Filling for Vapor Adsorption. *J. Colloid Interface Sci.* **1966**, *21*, 378–393. DOI: 10.1016/0095-8522(66)90004-3.

[50] Gallego-Juarez, J.; Graff, K., Eds. *Power Ultrasonics: Applications of High-Intensity Ultrasound*, 1st ed.; Woodhead Publishing, Cambridge, UK, **2015**.

[51] Breitbach, M.; Bathen, D. Influence of Ultrasound on Adsorption Processes. *Ultrason. Sonochem.* **2001**, *8*, 277–283. DOI: 10.1016/S1350-4177(01)00089-X.

[52] Naji, O.; Al-Juboori, R. A.; Bowtell, L.; Alpatova, A.; Ghaffour, N. Direct Contact Ultrasound for Fouling Control and Flux Enhancement in Air-Gap Membrane Distillation. *Ultrason. Sonochem.* **2020**, *61*, 104816. DOI: 10.1016/j.ultsonch.2019.104816.

[53] Labouret, S.; Frohly, J. Determination of Bubble Size Distributions in an Ultrasonic Cavitation Field. *J. Acoust. Soc. Am.* **2010**, *127*, 1984–1984. DOI: 10.1121/1.3385105.

[54] Merouani, S.; Hamdaoui, O.; Rezgui, Y.; Guemini, M. Energy Analysis during Acoustic Bubble Oscillations: Relationship between Bubble Energy and Sonochemical Parameters. *Ultrasonics.* **2014**, *54*, 227–232. DOI: 10.1016/j.ultras.2013.04.014.

[55] Lee, G. L.; Law, M. C.; Lee, V. C.-C. Modelling of Liquid Heating Subject to Simultaneous Microwave and Ultrasound Irradiation. *Appl. Therm. Eng.* **2019**, *150*, 1126–1140. DOI: 10.1016/j.applthermaleng.2019.01.064.

[56] Bulliard-Sauret, O.; Berindei, J.; Ferrouillat, S.; Vignal, L.; Memponteil, A.; Poncet, C.; Leveque, J. M.; Gondrexon, N. Heat Transfer Intensification by Low or High Frequency Ultrasound: Thermal and Hydrodynamic Phenomenological Analysis. *Exp. Therm. Fluid Sci.* **2019**, *104*, 258–271. DOI: 10.1016/j.expthermflusci.2019.03.003.